#### Volaric MP, Berg P, Reidenbach MA. Drivers of Oyster Reef Ecosystem Metabolism Measured Across Multiple Timescales. Estuaries and Coasts. 2020 May 11:1-2. DOI: doi.org/10.1007/s12237-020-00745-w

Oyster reef metabolism

# Drivers of Oyster Reef Ecosystem Metabolism Measured Across

**Multiple Timescales** 6 7 Martin P. Volaric\*, Peter Berg, and Matthew A. Reidenbach Department of Environmental Sciences, University of Virginia, Charlottesville, Virginia 22904, USA 

\*Corresponding Author: mpv3a@virginia.edu, 571-451-5865

### Abstract

Oxygen flux measurements between oyster reefs and the overlying water column
approximate total ecosystem metabolism, representing a potentially valuable reef monitoring tool.
In this study, seasonal oxygen flux measurements were made over an intertidal Crassostrea
virginica oyster reef on the Virginia (USA) coast using the non-invasive aquatic eddy covariance
(AEC) technique. Reef respiration (R) ranged from -276 mmol m <sup>-2</sup> d <sup>-1</sup> in the summer to -55 mmol
m <sup>-2</sup> d <sup>-1</sup> in the winter, likely due to temperature effects on oyster filtering and sediment microbial
activity. Reef gross primary production (GPP) varied less seasonally, resulting in net ecosystem
metabolism (NEM) that was highly heterotrophic in the summer (-141 mmol m <sup>-2</sup> d <sup>-1</sup> ) and nearly
balanced in the winter (-11 mmol m <sup>-2</sup> d <sup>-1</sup> ). Measurements of reef sediment chl a indicated higher
concentrations of benthic microalgae than surrounding bare mudflat, while photosynthesis -
irradiance curves utilizing 15 min flux averages confirmed light as a dominant short-term driver
of microalgal production. Metabolic values were compared to past AEC results from this reef,
creating a four-year record that included a significant oyster die-off. Over this time span R was
closely coupled to GPP, indicating rapid internal cycling of carbon, while reef primary production
was primarily attributed to sediment, rather than epiphytic, microalgae. Both R and GPP
substantially decreased following the oyster die-off. These results illustrate that oyster reefs are
highly dynamic environments, with complex processes that act on numerous time scales ranging
from minutes to years. Consequently, AEC metabolism measurements can aid in oyster reef
monitoring.

KEY WORDS: Crassostrea virginica, Oxygen flux, Benthic microalgae, primary production

#### INTRODUCTION

Oyster reefs are vital coastal systems that provide habitat for a wide range of organisms and improve overall water quality (Cohen et al. 2007). Unfortunately, due to a combination of overharvesting (Jackson et al. 2001) and disease (Oliver et al. 1998; Rothschild et al. 1994), oyster populations have declined by 85% globally below 19<sup>th</sup> century levels (Beck et al. 2011). As a result, oyster reefs have become the focus of many restoration efforts, including successful restorations in both North America and Europe (Beck et al. 2011).

Due to their importance to coastal systems, and to the high cost of restoration, oyster reef monitoring techniques have long been the subject of much research (e.g. Coen and Luckenbach 2000). One attribute of oyster reefs that has recently been studied in more detail is their consumption and daytime production of oxygen, which have been measured for reefs under a wide range of ambient nutrient levels (Kellogg et al. 2013; Reidenbach et al. 2013; Humphries et al. 2016; Casas et al. 2018; Volaric et al. 2018). Much of this previous work has focused on oxygen flux in relation to nitrogen cycling, as oxygen uptake by oyster reefs is positively correlated with denitrification (Kellogg et al. 2013, 2014; Humphries et al. 2016; Smyth et al. 2016). Oxygen flux can also be used as a proxy for whole-system heterotrophic activity and primary production (Glud, 2008). Oyster reefs are complex communities, containing numerous benthic infauna (Rodney and Paynter 2006) and micro- and macroalgae (Thomsen and McGlathery 2006). By integrating over this entire ecosystem, oxygen flux measurements provide key insight into whole-reef functioning, and if measured *in situ*, allow for the identification of environmental drivers that stimulate reef activity.

Recent studies of oxygen flux over oyster reefs have primarily relied on chamber incubations, both *ex situ* (Kellogg et al. 2013, 2014; Smyth et al. 2016; Casas et al. 2018) and *in* 

situ (Humphries et al. 2016), or on the *in situ* aquatic eddy covariance (AEC) technique (Reidenbach et al. 2013, Volaric et al. 2018). Chamber measurements isolate a small portion (< 1 m²) of the reef and overlying water column to create a well-defined control volume, determining the flux as the change in dissolved oxygen over time. In doing so, chambers either interfere with or disregard natural environmental conditions that can vary substantially (Reidenbach et al. 2013, Volaric et al. 2018). AEC measurements represent an adaptation of a technique long-used in the atmosphere (Priestly and Swinbank 1947), and have several advantages over traditional flux methods. In addition to yielding the integrated flux over a large benthic surface (often > 100 m²; Berg et al. 2007) under minimally invasive *in situ* conditions (Berg et al. 2003, Lorrai et al. 2010), they also have a high temporal resolution over long continuous deployments (providing 15 min flux values over 24-72 h intervals; Volaric et al. 2018), which allows for the calculation of fluxes over tidal and daily timescales.

Past studies of oyster reef oxygen flux have demonstrated the substantial impact of the physical environment on reef functioning. *In situ* AEC studies have shown that both flow speed and light are key drivers of reef metabolism, while respiration increases proportionally with oyster density (Reidenbach et al. 2013; Volaric et al. 2018). Both AEC and chamber studies have demonstrated greater oxygen flux towards the reef during dark vs. light conditions due to benthic primary production, with this production also scaling with oyster density (Kellogg et al. 2014; Volaric et al. 2018). However, less is known about longer term drivers of oyster reef oxygen dynamics over seasonal and interannual timescales. Recent chamber measurements have demonstrated higher nighttime uptake in the summer vs. the spring and fall (Kellogg et al. 2013; Humphries et al. 2016), while to date there has only been one previous study of winter oyster reef oxygen flux, which measured the difference in dissolved oxygen on two ends of an *in situ* 

plexiglass flow-through tunnel (Dame et al. 1992). This previous study found a net release of oxygen in the winter, which was attributed to the appearance of macroalgae that was not present in other seasons. To our knowledge there have been no studies that have measured the metabolism of a single oyster reef across multiple years.

Given these past results and knowledge gaps, the goal of this study was to identify drivers of oyster reef oxygen flux across multiple timescales, ranging from 15 minutes to interannual. To do this, we made seasonal (spring, summer, fall, winter) AEC measurements over an intertidal oyster reef over 1 year (fall 2016 – summer 2017), as well as the following summer (2018). We then combined our results with summer and fall AEC data from 2015 and 2016 at this same site (Volaric et al. 2018), establishing a four-year record of oyster reef oxygen fluxes. Over the course of this four-year period the reef experienced an unexpected and significant die-off in oysters. As a result, this interannual record describes the metabolism of the reef across a range of health and oyster densities, and allows us to quantify the impact of this die-off on reef metabolic function.

#### **METHODS**

#### Study site and sampling protocol

The study site was a natural intertidal eastern oyster *Crassostrea virginica* reef measuring 240 m<sup>2</sup> in size (22.5 m long x 10.5 m wide), with a water depth at high tide of approximately 1-1.5 m. It was located within the Hillcrest Oyster Sanctuary, a network of intertidal oyster reefs monitored by The Nature Conservancy along Virginia's Eastern Shore. This sanctuary is contained within the Virginia Coast Reserve (VCR), part of the National Science Foundation's Long-Term Ecological Research (LTER) network.

In order to quantify seasonal variations in oyster reef metabolism, we made aquatic eddy covariance (AEC) and sediment chl a measurements each season over one calendar year.

124

125

126

127

128

129

130

131

132

133

134

135

136

137

138

139

140

141

142

143

Sampling dates were as follows: October 26-November 3, 2016 (fall), January 12-20, 2017 (winter), April 12-April 21, 2017 (spring), and July 21-July 28, 2017 (summer). AEC measurements were also made the following summer, from June 7-June 16, 2018.

#### **Equipment and observation setup**

AEC measurements were made using a Nortek AS Vector<sup>©</sup> acoustic Doppler velocimeter (ADV) connected to a fast-response (90% response time ≤ 0.4 s) oxygen micro-sensor via a specially designed high-resolution amplifier (Fig. 1). For fall - summer 2016-2017 seasonal measurements Unisense AS Clark-type oxygen microelectrodes were used, while summer 2018 measurements utilized PreSens eddy covariance micro-optodes. Prior to deployment a specialized alignment tool was attached to the ADV in order to visualize its measurement volume, which consists of a cylinder approximately 14 mm in diameter and 14 mm in height. The oxygen microsensor was placed 0.5 cm from the edge of this volume to avoid interference with ADV data collection. The ADV, amplifier, and micro-sensor were powered by the same external battery, and were mounted together on a minimally-invasive stainless-steel frame (Fig. 1). Together these sensors measured the three-dimensional velocity and oxygen concentration at 32 Hz over 15 min bursts, with each burst consisting of 14.5 min of data collection followed by a 0.5 min pause. The measurement height for all deployments was set to ~10 cm above the reef (defined by the tops of oyster shells), a distance that was chosen to balance the smoothing of heterogeneity effects (Rheuban and Berg 2013) against the need to maximize data collection intervals in this intertidal system. Only data recorded when both the Vector and oxygen micro-sensor were submerged were used for further analysis, which at this site occurred approximately 4-6 h per tidal cycle or 8-12 h per day. The data contained some additional gaps due to sensor breakage and/or malfunction (see below). In total, 244 h of high-quality AEC data were selected for further analysis.

In order to calibrate the oxygen micro-sensors, and to measure water temperature, PME miniDOT $^{\odot}$  stable oxygen optodes were placed close to the eddy systems. Underwater photosynthetically active radiation (PAR) was measured at the same depth as the AEC measurement volume using Odyssey loggers that were calibrated as described in Long et al. (2012). Benthic chl a was determined for the top 1 cm of reef sediments using a methanol-acetone extraction combined with a Shimadzu UV 1800 spectrophotometer (Lorenzen 1967). Sediment samples for chl a were collected once per season concurrent to AEC measurements. Equal replicates were collected from both the ebb and flood sides of the AEC system (described below), as well as from an adjacent mudflat to act as a control.

#### **AEC** data analysis

To reduce noise, the 32 Hz data collected by the ADV were averaged down to 8 Hz (Berg et al. 2009). These 8 Hz data, separated into 15 min bursts, were used to calculate the oxygen flux between the reef and the water column as:

$$\overline{J_{O_2}} = \overline{w'C'} \tag{1}$$

where  $J_{O_2}$  is the oxygen flux, w' and C' are the instantaneous fluctuations away from the means of the vertical velocity and oxygen concentration, respectively, and the overbars indicate time averaging (Berg et al. 2003). This calculation was performed using the software package EddyFlux Ver 3.00 (P. Berg, unpubl.). Velocity and oxygen concentration means for  $\sim 90\%$  of the 15 min bursts were determined via a least-squares linear fit to the 8 Hz data (Lee et al. 2004; Berg et al. 2009), while the remaining  $\sim 10\%$  of bursts showed signs of non-linear large-scale fluctuations in oxygen concentration that were not attributable to turbulent eddies. Means for these bursts were determined using a 90 s running average (Lee et al. 2004; Volaric et al. 2018). Each 15 min burst was examined for possible sensor malfunctions including data spikes, excessive signal noise, or

abrupt variation from the miniDOT oxygen signal (Lorrai et al. 2010). Any data that showed signs of these anomalies were removed. Small-wave activity, identifiable by sinusoidal-like variations in the velocity data, was observed during part of data collection. As a result, no time-shift was applied to the oxygen data when calculating the flux, as time-shifting under wavy conditions can severely bias AEC flux calculations (Berg et al. 2015; Reimers et al. 2016).

Following data quality control, each 15 min flux was categorized as either daytime or nighttime based on PAR (nighttime values < 1% maximum PAR, daytime values > %1 maximum PAR). In order to calculate seasonal photosynthesis-irradiance (P-I) relationships, as well as test for possible light saturation, daytime data were fit with a hyperbolic tangential function of the form (Jassby and Platt 1976, Rheuban et al. 2014):

$$J_{O_2} = P_{max} \tanh \frac{PAR}{PAR_S} - R_I \tag{2}$$

where  $P_{max}$ ,  $PAR_S$ , and  $R_I$  are fitting parameters representing the maximum photosynthetic rate, saturating light level, and respiration, respectively. If no light saturation occurs, the hyperbolic tangential function converges to a line.

Ecosystem respiration (R) was defined as the mean nighttime flux. Due to the intertidal nature of the site, we could not collect continuous 24 h eddy flux data. Therefore, in order to calculate gross primary production (GPP) and net ecosystem metabolism (NEM), we created composite 24 h days using the mean flux values of specific hours (e.g. 9am – 10am, 10am – 11am, etc.) collected for each season (Volaric et al. 2019). For nighttime hours with no data, we estimated the mean hourly flux as the mean nighttime flux. For daytime hours with no data, we estimated the mean hourly flux using the P-I relationship for that season with PAR that was linearly interpolated based on adjacent mean hourly PAR. Using these composite 24 h days we calculated GPP and NEM as (Hume et al. 2011, Volaric et al. 2019):

$$GPP = \frac{1}{24} \left( \sum flux_{LIGHT} + \frac{|\sum flux_{DARK}|}{h_{DARK}} h_{LIGHT} \right)$$
 (3)

$$NEM = \frac{1}{24} \left( \sum flux_{LIGHT} + \sum flux_{DARK} \right)$$
 (4)

- where  $h_{LIGHT}$  and  $h_{DARK}$  are the number of hours out of 24 that were predominantly light or dark,
- respectively, for each season, and  $flux_{LIGHT}$  and  $flux_{DARK}$  are the mean fluxes during those hours.
- Due to the interpolation of a small number of hourly values for each season we did not assign
- error to NEM or GPP, and these values represent point estimates.
- We additionally calculated the Q<sub>10</sub> value for reef R, defined as the proportional change in
- 197 response to a 10°C increase in temperature, using an exponential fit to the seasonal R vs. water
- temperature (T) relationship (Lloyd and Taylor 1994, Pederson et al. 2016):

$$R = A * \exp(B * T) \tag{5}$$

- where A and B are fitting parameters and  $B = \frac{lnQ_{10}}{10}$ . For this calculation, the seasonal mean
- 201 nighttime water temperature was determined using miniDOT data.

#### **AEC** measurement footprint and reef density

202

- The AEC footprint is defined as the elliptical benthic surface area upstream of the system
- 204 that contributes to the recorded oxygen flux (Berg et al. 2007). For this reef, the upstream distance
- 205 that encompasses 80% of the flux contribution was previously estimated as 12 m (Volaric et al.
- 206 2018). Due to tidal flow over the reef, the footprint recorded during flood tide measurements is
- different than that measured during ebb tide measurements, with these two footprints being on
- 208 opposite sides of the AEC system (Fig. 1).
- In order to account for possible differences in oyster density between the footprints,
- replicate (n = 4-12) density counts were made within both flood and ebb tide footprints during
- seasonal AEC measurements. All counts were of adult oysters with shell length > 50 mm using a
- 212 0.5 m x 0.5 m quadrat placed randomly within the approximate area of each footprint.

#### Interannual reef metabolism

In order to create a four-year interannual record of reef metabolism, seasonal 2016-2017 and summer 2018 values of R, GPP, and NEM were compared to past AEC measurements by Volaric et al. (2018). For this comparison we calculated GPP and NEM for these past data as described in Eq. 3 and Eq. 4. These previous measurements occurred during summer and fall 2015, and summer 2016.

#### **RESULTS**

#### Reef density and oyster die-off

In summer 2015, the density of the entire reef, including both flood and ebb tide footprints, was  $350 \pm 62$  oysters  $m^{-2}$  (mean  $\pm$  SE, n=4; Volaric et al. 2018). Oyster density was not significantly different (t=1.0, p=0.33) in summer 2016, at which time it was measured as 244  $\pm$  61 oysters  $m^{-2}$  (n=10). There was an apparent oyster die-off between summer and fall 2016, as from fall 2016 - summer 2017 the density of the reef was  $111 \pm 17$  oysters  $m^{-2}$  (n=44). This die-off was more pronounced within the ebb tide measurement footprint than the flood tide footprint (Fig. 1). As a result, oyster density was significantly (t=2.11, p=0.04) greater in the flood vs. ebb tide footprint, with means of  $137 \pm 13$  (n=22) and  $92 \pm 17$  (n=22) oysters  $m^{-2}$ , respectively. Oyster density was not significantly different between seasons (one-way ANOVA, p=0.56), so density counts from fall 2016 through summer 2017 were grouped together. Differences between ebb and flood tide density were not evident in summer 2018, at which time the density of the reef was  $103 \pm 27$  oysters  $m^{-2}$  (n=12).

#### Seasonal patterns of metabolism

During fall 2016 – summer 2017 seasonal measurements, nighttime oxygen flux was consistently greater in the flood tide footprint than the ebb tide footprint (Fig. 2A). Both footprints

had nearly equal nighttime flux per oyster, signifying that this difference in uptake was due to differences in oyster density (Fig. 2). Given that there were approximately equal flood and ebb tide nighttime flux measurements for each season (Fig. 2A), flood and ebb tide flux values were grouped when calculating seasonal R below.

Photosynthesis-irradiance (P-I) relationships show that light had a significant impact on reef metabolism by stimulating microalgal photosynthesis in all seasons (Fig. 3). For summer data the hyperbolic tangential function converged to a linear relationship, indicating a lack of light saturation. These P-I curves allow for the prediction of the seasonal reef light compensation point (x-intercept), which ranged from a low of 127  $\mu$ mol photons m<sup>-2</sup> s<sup>-1</sup> in the winter to a high of 1019 photons m<sup>-2</sup> s<sup>-1</sup> in the summer.

Composite 24 h days from each season, used to calculate GPP and NEM, are presented in Fig. 4. This figure demonstrates the strong relationship between oxygen production and PAR, particularly during the summer (Fig. 4D), which showed a relatively high release (~ 300 mmol m<sup>-2</sup> d<sup>-1</sup>) of oxygen during the high-light mid-day hours.

Seasonal metabolism values from fall 2016 through summer 2017 are presented in Fig. 5. R showed significant seasonal variation (one-way ANOVA, p < 0.01), with Tukey HSD post-hoc tests indicating significant (p < 0.01) differences between all seasons, with the exception of fall and spring. GPP showed little seasonal variation with the exception of summer, which was substantially greater than the other seasons. NEM varied considerably seasonally, from a nearly balanced state in winter to strong net heterotrophy in the summer (Fig. 5D). Mean nighttime water temperature was 16.3, 5.9, 16.8, and 25.9 °C during fall, winter, spring, and summer measurements, respectively, resulting in a Q<sub>10</sub> value of 2.2.

Benthic chl a showed a significant (one-way ANOVA, p < 0.01) seasonal signal, with a high of  $146 \pm 13$  (mean  $\pm$  SE, n = 4) mg m<sup>-2</sup> in the fall and a low of  $84 \pm 8$  (n = 10) mg m<sup>-2</sup> in the winter, and intermediate values in the spring and summer (Fig. 6). With the exception of fall, values were significantly (p < 0.01) greater over the oyster reef than over the mudflat, which showed a similar seasonal pattern as the reef. There was no significant difference between chlorophyll samples collected in the flood tide footprint vs. the ebb tide footprint, and samples were combined in these results.

#### **Interannual metabolism**

Seasonal 2016-2017 and summer 2018 AEC measurements were compared to past values from this same oyster reef taken during summer and fall 2015, and summer 2016 (Volaric et al. 2018), creating a four-year interannual record of metabolism. Both R and GPP significantly decreased following an oyster die-off in late summer 2016, and were highly correlated to one another ( $R^2 = 0.89$ ) across this 4 year-period (Fig. 7). This R vs. GPP relationship fell below a 1-to-1 line, indicating net heterotrophy.

Summer values of R, GPP, and NEM vs. oyster density are presented in Fig. 8. Included in this analysis are summer values from the reef in 2015, 2016, 2017, and 2018, as well as summer metabolism values from two different nearby oyster reefs sampled within Volaric et al. (2018). Additionally, summer 2017 flood and ebb tide R values (Fig. 2A) were both included in the R vs. density relationship (Fig. 8A). Oyster density was strong control of both R (p < 0.01,  $R^2 = 0.84$ ) and NEM (p < 0.01,  $R^2 = 0.96$ ), but had only a weak, non-significant impact on GPP (p = 0.20,  $R^2 = 0.37$ ).

#### **DISCUSSION**

This study represents the most comprehensive collection of AEC metabolism data to date for an oyster reef. Unlike chamber measurements, our data were all collected under true *in situ* conditions – exposed to natural variations in flow speed, tidal stage, light, temperature, and suspended sediment concentration. However, given the intertidal nature of the site, these values only apply to times when the reef was submerged, which includes approximately half of each day (Reidenbach et al. 2013; Volaric et al. 2018). They do not account for benthic activity that occurs during air-exposed conditions.

One way to develop a first-order estimate of the true 24 h reef metabolism, including both submerged and emergent conditions, is to assume that GPP closely approximates true daily values, while oyster respiration is absent when the reef is exposed. Algal photosynthesis in intertidal systems is often assumed to be similar during submerged vs. emergent conditions (Barranguet et al. 1998; Volaric et al 2019), while sediment and microalgal R are also nearly equivalent (Barranguet et al. 1998). Therefore, the main change to reef metabolism during exposure is the loss of oyster respiration. This loss can be accounted for by recalculating R as the weighted average based on exposure time between sediment R and total reef R, then calculating NEM as modified R + GPP. Given our interannual record, we are able to estimate sediment and microalgal R during summer months (described below). Using this revised methodology, full 24 h estimates for summer 2017 R, GPP and NEM are -194, 126, and -68 mmol m<sup>-2</sup> d<sup>-1</sup>, respectively.

#### Seasonal drivers of oyster reef metabolism

Seasonality substantially impacted oyster reef metabolism, as R varied significantly between winter, summer, and spring/fall (Fig. 5). These differences appear to be driven by seasonal changes in heterotrophic, rather than autotrophic, activity, as the difference between

summer and winter R (221 mmol m<sup>-2</sup> d<sup>-1</sup>) was nearly 3x greater than the difference in GPP (85 mmol m<sup>-2</sup> d<sup>-1</sup>; Fig. 5). Our results agree with past studies of subtidal mussel beds, which also exhibit greater seasonal variation in R than in GPP (Attard et al. 2019). This difference in magnitude between heterotrophic and autotrophic seasonality may be partially explained by water depth, which can impact benthic production by increasing light attenuation (Koweek et al. 2018). Maximum water depth, measured at a nearby tidal station, was approximately 30 cm greater in the summer than in the winter (Porter et al. 2019a), which likely muted seasonal effects on GPP while having little to no impact on R. Instead, seasonal changes to R are likely driven by water temperature, as temperature increases have been shown to stimulate both bacterial activity (Apple et al. 2006), and oyster filtering and oxygen consumption (Shumway and Koehn 1982; Haure et al. 1998). Mean nighttime water temperature over each sampling period ranged from a low of 6 °C in the winter to a high of 26 °C in the summer, with approximately equal temperatures in the spring and fall (16-17 °C). The Q<sub>10</sub> value for reef R was 2.2, which agrees with the range of 2 - 4 previously determined for oyster reefs (Boucher and Boucher-Rodini 1988).

The difference in the magnitude of seasonal effects between R and GPP is reflected in NEM values, which ranged from strongly heterotrophic in the summer, when R was highest, to nearly balanced in the winter, when R was lowest (Fig. 5). As a result, the light compensation point for the reef was highest in the summer, lowest in the winter, and intermediate in the spring and fall (Fig. 3). Fall, winter, and spring P-I curves all showed signs of light saturation, which is typical for aquatic primary production (Binzer et al. 2006). The summer P-I relationship converged to a line, despite experiencing the highest light levels (Fig. 3D), indicating a lack of light saturation. Therefore, although GPP showed relatively little seasonal variation, P-I relationships suggest that photosynthetic production was light limited during the summer but not

for other seasons. This result agrees with past studies, as the light saturation point of intertidal sediments is positively correlated with temperature (Barranguet et al. 1998), likely due to its effects on microbial primary production (Apple et al. 2006).

During winter measurements a green, filamentous, algae was seen coating the oyster shells (Fig. 9). Dame et al. (1992) observed a similar biofilm during their winter measurements of oyster metabolism, which they correlated to large values of winter reef primary production. In our study autotrophic activity on the reef showed relatively little seasonal variation (Fig. 5), however, the source of this production likely differed between this ephemeral epiphytic green alga during the winter, and sediment microalgae during the spring, summer, and fall. Not only was sediment chl *a* on the reef lowest in the winter (Fig. 6), indicating a seasonal minimum of benthic microalgae, but cold winter water temperatures suggest that these benthic algae were also less productive on a per-area basis (Apple et al. 2006). This seasonal shift in the source of production likely alters biomass turnover rates, which in turn can impact food web dynamics and biogeochemical cycling (McGlathery et al. 2007; Attard et al. 2019).

#### Interannual and sediment metabolism

Our interannual record demonstrates extremely high rates of benthic activity, particularly before the oyster die-off. The maximum R we recorded when the reef was submerged was -511 mmol m<sup>-2</sup> d<sup>-1</sup> (Fig. 7A), which approaches the respiration of subtidal tropical coral reefs (-566 mmol m<sup>-2</sup> d<sup>-1</sup>; Long et al. 2013). Similarly, maximum GPP was 220 mmol m<sup>-2</sup> d<sup>-1</sup>, which falls at the lower end of the range of values measured over dense seagrass meadows (~200 - 400 mmol m<sup>-2</sup> d<sup>-1</sup>; Berger et al 2020).

Summer values of R were consistently greater than GPP (Fig. 7), and although GPP was only weakly correlated, both were proportional to oyster density (R:  $R^2 = 0.84$ , GPP:  $R^2 = 0.37$ ;

350

351

352

353

354

355

356

357

358

359

360

361

362

363

364

365

366

367

368

369

370

371

Fig. 8), agreeing with past studies of oyster metabolism (Kellogg et al. 2014; Volaric et al. 2018). As R was greater than GPP, summer NEM was always negative (Fig. 8C) and the GPP vs. R relationship fell below a 1-to-1 line (Fig. 7B), indicating net heterotrophy. This means the reef requires external sources of carbon, which likely come from water column phytoplankton and detritus consumed by the oysters.

Our multi-year record of summertime reef metabolism also allows us to estimate summertime sediment activity on the reef. Conceptually, the slope of the best fit line in Fig. 8A (R vs. oyster density) represents a first-order estimate of the summer respiration contribution per oyster, including any encrusting microorganisms, while the v-intercept (-112  $\pm$  50 mmol m<sup>-2</sup> d<sup>-1</sup>) is a first-order estimate of the respiration of reef sediments alone. As total reef R in summer 2017 was -276 mmol m<sup>-2</sup> d<sup>-1</sup> (Fig. 5A), approximately 40% of the heterotrophic activity on the reef during this time can be attributed to sediment bacteria, algae and infauna, while the remaining 60% (-164 mmol m<sup>-2</sup> d<sup>-1</sup>) can be attributed to oysters and associated encrusting microorganisms. This estimate agrees with Boucher and Boucher-Rodini (1988), who measured the oxygen flux of transplanted C. gigas oysters and sediments using in situ dark enclosure incubations. Correcting their values for our reef density also results in contributions of 60% by oysters and 40% by reef sediments. Our results also closely agree with Casas et al. (2018), who measured the oxygen uptake of scrubbed (i.e. all epiphytes removed) oysters in dark chamber incubations. Multiplying their per oyster values by the reef density gives a total oyster respiration of -173 mmol m<sup>-2</sup> d<sup>-1</sup>. This value is nearly identical to our first-order estimate, indicating that there was likely negligible epiphytic activity during summer measurements. However, this was probably not the case in the winter, when epiphytic algae were abundant on oyster shells (Fig. 9). Given that there was

minimal macroalgae observed on the reef during measurement intervals, these results suggest that summer reef GPP is dominated by sediment microalgal production.

Values of R and GPP were strongly correlated across the 4 years of measurements for this reef (Fig. 7). A similar coupling has been demonstrated in mussel beds, where ~50 % of annual R is attributed to autochthonous carbon (Attard et al. 2019), and is explained by an efficient recycling of carbon. Oysters can feed on benthic diatoms that have been suspended into the water column by waves or water currents (Kasim and Mukai 2006), so enhanced production by benthic algae may lead to higher oxygen consumption by oysters. Likewise, nitrogen waste from oysters can stimulate sediment microalgal growth (Kellogg et al. 2014), which may also explain why sediment microalgal concentrations were significantly greater on the reef than an adjacent mudflat (Fig. 6).

#### Oxygen flux as a tool for oyster reef monitoring

Although there is some debate regarding which ecosystem services are enhanced by oyster restoration (Coen et al. 2007), our four-year record demonstrates that oyster reefs are metabolic hotspots that exhibit strong positive correlations between ecosystem metabolism and oyster density (Fig. 8). Due to this relationship, we were able to show ecosystem-wide effects of an oyster die-off on this reef, which resulted in significant decreases to both R and GPP (Fig. 7). The die-off appears to have occurred between July and October 2016, but its cause is uncertain and likely multifactorial. One possible explanation is heat stress during late summer 2016. Extended periods of elevated air temperatures > 30 °C have been shown to increase the mortality of juvenile intertidal *C. virginica* oysters (Roegner and Mann 1995). Nearby hourly data demonstrate that there were 13 days in August 2016 with maximum temperatures above 30 °C, while there were only 3 such days in August 2015 (Porter et al. 2019b).

Unlike traditional monitoring methods focused on oyster density and recruitment (Coen and Luckenbach 2000), AEC measurements provide valuable insight into the health, function, and biodiversity of the entire benthic community (Rodil et al. 2019). For oyster reefs this community includes reef microalgae, which due to their ubiquity in coastal environments, combined with their rapid response to changes in water quality, have been proposed as a potentially valuable bioindicator in marine environments (Desrosiers et al. 2013). By quantifying rates of benthic primary production, oxygen flux acts as a proxy for the activity of these microorganisms. This proxy, combined with R values that can largely (~60%) be attributed to oyster activity, allows for the near-instantaneous approximation of the health and activity of the entire reef community. As a result, measurements of oxygen flux can potentially demonstrate severe reef distress before other signs such increases in mortality or decreases in recruitment are detected by resource managers, and are a valuable addition to reef monitoring efforts.

Acknowledgements: We would like to thank B. Lusk and The Nature Conservancy for providing access to the site as well as background information on the oyster reefs. We would also like to thank D. Boyd, D. Lee, and E. Stine for field assistance, as well as L. Aoki and M. Miller for laboratory assistance. Support for this study was provided by the National Science Foundation (NSF) through grants for the Virginia Coast Reserve Long-Term Ecological Research program (DEB-1237733 and DEB-1832221), Chemical Oceanography program (OCE-1334848) to P. Berg, and a CAREER Grant to M. A. Reidenbach (OCE-1151314). Support was also provided by the University of Virginia.

416	Works Cited
417	Apple, J.K., P.A. del Giorgio, and W.M. Kemp. 2006. Temperature regulation of bacterial
418	production, respiration, and growth efficiency in a temperate salt-marsh estuary. Aquatic
419	Microbial Ecology 43: 243-255. https://doi.org/10.3354/ame0403243
420	Attard, K.M., I.F. Rodil, R.N. Glud, P. Berg, J. Norkko, and A. Norkko. 2019. Seasonal
421	metabolism across shallow benthic habitats measured by aquatic eddy covariance.
422	Limnology and Oceanography: Letters: 2019. https://doi.org/10.1002/lol2.10107
423	Barranguet, C., J. Kromkamp, and J. Peene. 1998. Factors controlling primary production and
424	photosynthetic characteristics of intertidal microphytobenthos. Marine Ecology Progress
425	Series 173: 117-126. https://doi.org/10.3354/meps173117
426	Beck, M.W, R.D. Brumbaugh, L. Airoldi, A. Carranza, L.D. Coen, C. Crawford, O. Defeo, G.J.
427	Edgar, B. Hancock, M.C. Kay, H.S. Lenihan, M.W. Luckenbach, C.L. Toropova, G.
428	Zhang, and X. Guo. 2011. Oyster reefs at risk and recommendations for conservation,
429	restoration, and management. Bioscience 61: 107-116,
430	https://doi.org/10.1525/bio.2011.61.2.5
431	Berg, P., H. Røy, F. Janssen, V. Meyer, B.B. Jørgensen, M. Huettel, and D. de Beer. 2003. Oxygen
432	uptake by aquatic sediments measured with a novel non-invasive eddy correlation
433	technique. Marine Ecology Progress Series 261: 75-83,
434	https://doi.org/10.3354/meps261075
435	Berg, P., H. Røy, and P. L. Wiberg. 2007. Eddy correlation flux measurements: the sediment
436	surface area that contributes to the flux. Limnology and Oceanography 52: 1672-1684.
437	https://doi.org/10.4319/lo.2007.52.4.1627

438	Berg, P., R.N. Glud, A. Hume, H. Stahl, K. Oguri, V. Meyer, and H. Kitazato. 2009. Eddy
439	correlation measurements of oxygen uptake in deep ocean sediments. Limnology and
440	Oceanography: Methods 7: 576-584. https://doi.org/10.4319/lom.2009.7.576
441	Berg, P., C.E. Reimers, J.H. Rosman, M. Huettel, M.L. Delgard, M.A. Reidenbach, and H.T.
442	Özkan-Haller. 2015. Technical note: Time lag correction of aquatic eddy covariance data
443	measured in the presence of waves. Biogeosciences 12: 6721-6735.
444	https://doi.org/10.5194/bg-12-6721-2015
445	Berger, A.C., P. Berg, K.J. McGlathery, and M.L. Delgard. 2020. Long-term trends and resilience
446	of seagrass metabolism: A decadal aquatic eddy covariance study. Limnology and
447	Oceanography 9999: 1-16. https://doi.org/10.1002/lno.11397
448	Binzer, T., K. Sand-Jensen, and A.L. Middelboe. 2006. Community photosynthesis of aquatic
449	macrophytes. Limnology and Oceanography 51(6): 2722-2733.
450	https://doi.org/10.4319/lo.2006.51.6.2722
451	Boucher, G., and R. Boucher-Rodoni. 1988. In situ measurement of respiratory metabolism and
452	nitrogen fluxes at the interface of oyster beds. Marine Ecology Progress Series 44: 229-
453	238. https://doi.org/10.3354/meps044229
454	Casas, S. M., R. Lavaud, M.K. La Peyre, L.A. Comeau, R. Filgueira, and J.F. La Peyre. 2018.
455	Quantifying salinity and season effects on eastern oyster clearance and oxygen
456	consumption rates. <i>Marine Biology</i> 165: 90. https://doi.org/10.1007/s00227-018-3351-x
457	Coen, L.D., and M.W. Luckenbach. 2000. Developing success criteria and goals for evaluating
458	oyster reef restoration: Ecological function or resource exploitation. Ecological
459	Engineering 15: 323-343. https://doi.org/10.1016/S0925-8574(00)00084-7

Coen, L.D., R.D. Brumbaugh, D. Bushkek, R. Grizzle, M.W. Luckenbach, M.H. Posev, S.P. 460 461 Powers, and S. Gregory Tolley. 2007. Ecosystem services related to oyster restoration. 462 Marine Ecology Progress Series 341: 303-307. https://doi.org/10.3354/meps341303 463 Dame, R.F., J.D. Spurrier, and R.G. Zingmark. 1992. In situ metabolism of an oyster reef. *Journal* 464 of Experimental Marine Biology and Ecology 164: 147-159. https://doi.org/10.1016/0022-465 0981(92)90171-6 466 Desrosiers, C., J. Leflaive, A. Eulin, and L. Ten-Hage. 2013. Bioindicators in marine waters: 467 Benthic diatoms as a tool to assess water quality from eutrophic to oligotrophic coastal 468 ecosystems. **Ecological Indicators** 32: 25-34. 469 https://doi.org/10.1016/j.ecolind.2013.02.021 470 Glud, R.N. (2008) Oxygen dynamics of marine sediments. Marine Biology Research 4: 243-289. 471 https://doi.org/10.1080/17451000801888726 472 Haure, J., C. Penisson, S. Bougrier, and J.P. Baud. 1998. Influence of temperature on clearance 473 and oxygen consumption rates of the flat oyster Ostrea edulis: determination of allometric 474 coefficients. Aquaculture 169: 211-224. https://doi.org/10.1016/S0044-8486(98)00383-4 475 Hume, A., P. Berg, and K.J. McGlathery. 2011 Dissolved oxygen fluxes and ecosystem 476 metabolism in an eelgrass (Zostera marina) meadow measured with the eddy correlation 477 Oceanography 86-96. technique. Limnology and 56: 478 https://doi.org/10.4319/lo.2011.56.1.0086 479 Humphries, A.T., S.G. Ayvazian, J.C. Carey, B.T. Hancock, S. Grabbert, D. Cobb, C.J. Strobel, 480 and R.W. Fulweiler. 2016. Directly measured denitrification reveals oyster aquaculture and 481 restored oyster reefs remove nitrogen at comparable high rates. Frontiers in Marine 482 Science 3: 74, https://doi.org/10.3389/fmars.2016.00074

483 Jackson, J.B.C., M.X. Kirby, W.H. Berger, K.A. Bjorndal, L.W. Botsford, B.J. Bourque, R.H. 484 Bradbury, R. Cooke, J. Erlandson, J.A. Estes, T.P. Hughes, S. Kidwell, C.B. Lange, H.S. 485 Lenihan, J.M. Pandolfi, C.H. Peterson, R.S. Steneck, M.J. Tegner, and R.R. Warner. 2001. 486 Historical overfishing and the recent collapse of coastal ecosystems. Science 293: 629-638, 487 https://doi.org/10.1126/science.1059199 488 Jassby, A.D., and T. Platt. 1976. Mathematical formulation of the relationship between 489 photosynthesis and light for phytoplankton. *Limnology and Oceanography* 21(4): 540-547. 490 https://doi.org/10.4319/lo.1976.21.4.0540 491 Kasim, M., and H. Mukai. 2006. Contribution of benthic and epiphytic diatoms to clam and oyster 492 production in the Akkeshi-ko estuary. Journal of Oceanography 62: 267-281, 493 https://doi.org/10.1007/s10872-006-0051-9 494 Kellogg, M.L., J.C. Cornwell, M.S. Owens, and K.T. Paynter. 2013. Denitrification and nutrient 495 assimilation on a restored oyster reef. Marine Ecology Progress Series 480: 1-19. 496 https://doi.org/10.3354/meps10331 497 Kellogg, M.L., J.C. Cornwell, M.S. Owens, M.W. Luckenbach, P.G. Ross, A.T. Leggett, J.C. 498 Dreyer, B. Lusk, A. Birch, and E. Smith. 2014. Scaling ecosystem services to reef 499 development: Effects of oyster density on nitrogen removal and reef community structure. 500 Science, College William Virginia Institute of Marine of & Mary. 501 https://doi.org/10.21220/V5G013 502 Koweek, D. A., R. C. Zimmerman, K. M. Hewett, B. Gaylord, S. N. Giddings, K. J. Nickols, J. L. 503 Ruesink, J. J. Stachowicz, Y. Takeshita, and K. Caldeira. 2018. Expected limits on the ocean acidification buffering potential of a temperate seagrass meadow. Ecological 504 505 *Applications* 28(7): 1694 – 1714. https://doi.org/10.1002/eap.1771

506	Lee, X., W. Massman, and B. Law. 2004. Handbook of Micrometeorology: A Guide for Surface
507	Flux Measurement and Analysis. Kluwer Academic Publishers, Dordrecht
508	Lloyd, J., and J.A. Taylor. 1994. On the temperature dependence of soil respiration. Functional
509	Ecology 8: 315-323. https://doi.org/10.2307/2389824
510	Long, M.H., J.E. Rheuban, P. Berg, and J.C. Zieman. 2012. A comparison and correction of light
511	intensity loggers to photosynthetically active radiation sensors. Limnology and
512	Oceanography: Methods 10: 416-424. https://doi.org/10.4319/lom.2012.10.416
513	Long, M.H., P. Berg, D. de Beer, and J.C. Zieman. 2013. In situ coral reef oxygen metabolism: an
514	eddy correlation study. <i>PLoS ONE</i> 8(3): e58581.
515	https://doi.org/10.1371/journal.pone.0058581
516	Lorrai, L., D.F. McGinnis, P. Berg, A. Brand, and A. Wüest. 2010. Application of oxygen eddy
517	correlation in aquatic systems. Journal of Atmospheric and Oceanic Technology 27: 1533-
518	1545. https://doi.org/10.1175/2010JTECHO723.1
519	Lorenzen, C.J. 1967. Determination of chlorophyll and pheo-pigments: spectrophotometric
520	equations. Limnology and Oceanography 12(2): 343-346.
521	https://doi.org/10.4319/lo.1967.12.2.0343
522	McGlathery, K.J., K. Sundback, and I.C. Anderson. 2007. Eutrophication in shallow coastal bays
523	and lagoons: The role of plants in the coastal filter. Marine Ecology Progress Series 348:
524	1-18. https://doi.org/10.3354/meps07132
525	Oliver, L.M., W.S. Fisher, S.E. Ford, L.M. Ragone Calvo, E.M. Burreson, E.B. Sutton, and J.
526	Gandy. 1998. Perkinsus marinus tissue distribution and seasonal variation in oysters
527	Crassostrea virginica from Florida, Virginia, and New York. Diseases of Aquatic
528	Organisms 34: 51-61. https://doi.org/10.3354/dao034051

529	Pederson, O., T.D. Colmer, J. Borum, A. Zavala-Perez, and G.A. Kendrick. 2016. Heat stress of
530	two tropical seagrass species during low tides - impact on underwater net photosynthesis,
531	dark respiration and diel in situ internal aeration. New Phytologist 210: 1207-1218.
532	https://doi.org/10.1111/nph.13900
533	Porter, J. H., D. O. Krovetz, J. Spitler, T. Williams, and K. Overman. 2019a. Tide data for Hog
534	Island (1991-), Redbank (1992-), Oyster (2007-). Environmental Data Initiative,
535	https://doi.org/10.6073/pasta/1d901718676ee95eccc575fdf641ff52. Dataset accessed
536	2/03/2020.
537	Porter, J.H., D.O. Krovetz, W. Nuttle, and J. Spitler. 2019b. Hourly meteorological data for the
538	Virginia Coast Reserve LTER 1989-present. Environmental Data Initiative,
539	https://doi.org/10.6073/pasta/63d9e078465f194dcf0296a8d52b7a04. Dataset accessed
540	3/29/2019.
541	Priestly, C., and W. Swinbank. 1947. Vertical transport of heat by turbulence in the atmosphere.
542	Proceedings of the Royal Society A 189: 543-561. https://doi.org/10.1098/rspa.1947.0057
543	Reidenbach, M.A., P. Berg, A. Hume, J.C.R. Hansen, and E.R. Whitman. 2013. Hydrodynamics
544	of intertidal oyster reefs: The influence of boundary layer flow processes on sediment and
545	oxygen exchange. Limnology and Oceanography: Fluids and Environments 3: 225-239.
546	https://doi.org/10.1215/21573689-2395266
547	Reimers, C.E., H.T. Özkan-Haller, and A.T. Albright. 2016. Microelectrode velocity effects and
548	aquatic eddy covariance measurements under waves. Journal of Atmospheric and Oceanic
549	Technology 33(2): 263-282. https://doi.org/10.1175/JTECH-D-15-0041.1

550	Rheuban, J.E., and P. Berg. 2013. The effects of spatial and temporal variability at the sediment
551	surface on aquatic eddy correlation flux measurements. Limnology and Oceanography:
552	Methods 11: 351-359. https://doi.org/10.4319/lom.2013.11.351
553	Rheuban, J.E., P. Berg, and K.J. McGlathery. 2014. Ecosystem metabolism along a colonization
554	gradient of eelgrass (Zostera marina) measured by eddy correlation. Limnology and
555	Oceanography 59(4): 1376-1387. https://doi.org/10.4319/lo.2014.59.4.1376
556	Rodil, I.F., K.M. Attard, J. Norkko, R.N. Glud, and A. Norkko. 2019. Towards a sampling design
557	for characterizing habitat-specific benthic biodiversity related to oxygen flux dynamics
558	using Aquatic Eddy Covariance. PLoS ONE 14(2): e0211673.
559	https://doi.org/journal.pone.0211673
560	Rodney, W.S., and K.T. Paynter. 2006. Comparisons of macrofaunal assemblages on restored and
561	non-restored oyster reefs in mesohaline regions of Chesapeake Bay in Maryland. Journal
562	of Experimental Marine Biology and Ecology 335: 39-51.
563	https://doi.org/10.1016/j.jembe.2006.02.017
564	Roegner, G.C., and R. Mann. 1995. Early recruitment and growth of the American oyster
565	Crassostrea virginica (Bivalvia: Ostreidae) with respect to tidal zonation and season.
566	Marine Ecology Progress Series 117: 91-101. https://doi.org/10.3354/meps117091
567	Rothschild, B.J., J.S. Ault, P. Goulletquer, and M. Heral. 1994. Decline of the Chesapeake Bay
568	oyster population: a century of habitat destruction and overfishing. Marine Ecology
569	Progress Series 111: 29-39. https://doi.org/10.3354/meps111029
570	Shumway, S.E., and R.K. Koehn. 1982. Oxygen consumption in the American Oyster Crassostrea
571	virginica. Marine Ecology Progress Series 9: 59-68. https://doi.org/10.3354/meps009059

572	Smyth, A.R., N.R. Geraldi, S.P. Thompson, and M.F. Piehler. 2016. Biological activity exceeds
573	biogenic structure in influencing sediment nitrogen cycling in experimental oyster reefs.
574	Marine Ecology Progress Series 560: 173-183. https://doi.org/10.3354/meps11922
575	Thomsen, M.S., and K.J. McGlathery. 2006. Effects of accumulations of sediments and drift algae
576	on recruitment of sessile organisms associated with oyster reefs. Journal of Experimental
577	Marine Biology and Ecology 328: 22-34. https://doi.org/10.1016/j.jembe.2005.06.016
578	Volaric, M. P., P. Berg, and M.A. Reidenbach. 2018. Oxygen metabolism of intertidal oyster reefs
579	measured by aquatic eddy covariance. Marine Ecology Progress Series 599: 75-91.
580	https://doi.org/10.3354/meps12627
581	Volaric, M. P., P. Berg, and M.A. Reidenbach. 2019. An invasive macroalga alters ecosystem
582	metabolism and hydrodynamics on a tidal flat. Marine Ecology Progress Series 628: 1-16.
583	https://doi.org/10.3354/meps13143

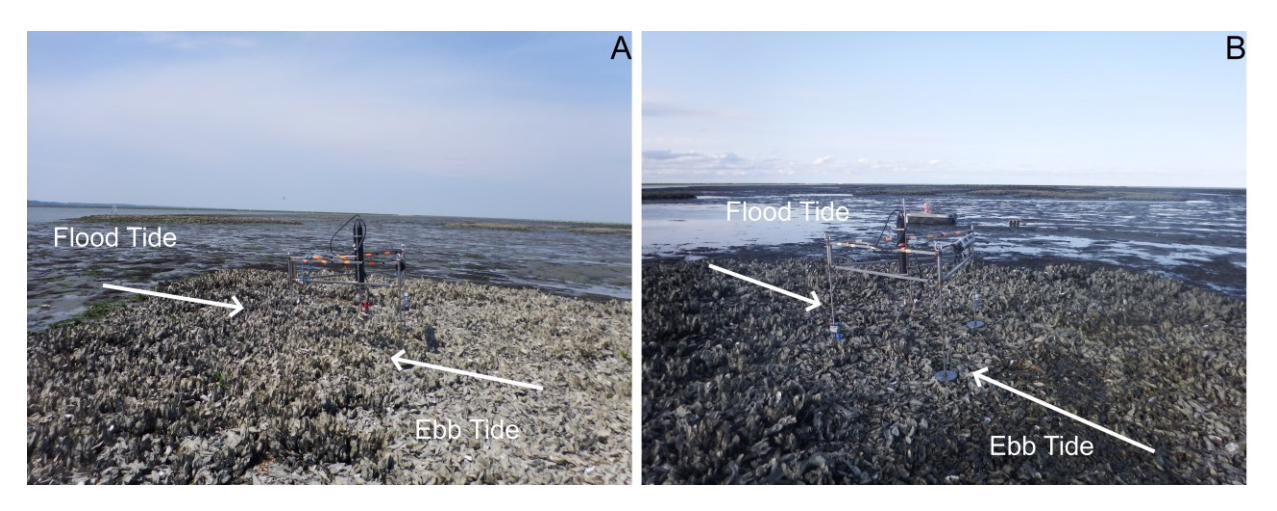


**Fig. 1** Aquatic eddy covariance system deployed on oyster reef during (A) June 2016 and (B) June 2017 measurements, showing approximate flow directions during both flood and ebb tides. Following an oyster die-off during late summer 2016, oyster densities in the flood tide measurement footprint were significantly higher than in the ebb tide footprint.

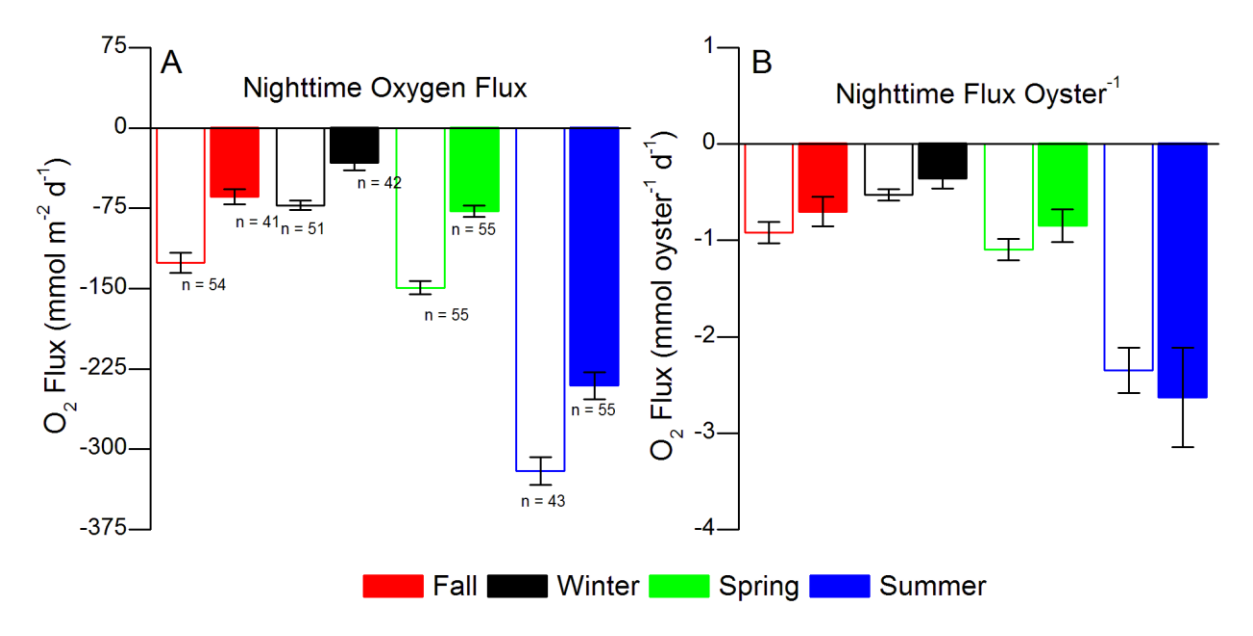


Fig. 2 Differences between flood tide (empty columns) and ebb tide (solid columns) (A) mean nighttime oxygen flux and (B) mean nighttime flux per oyster. Although mean nighttime flood and ebb tide flux were significantly (p < 0.01) different for each season, flux per oyster was approximately equal. Therefore, seasonal differences in nighttime flux between the two footprints are attributed to differences in oyster density. Bars represent SE.

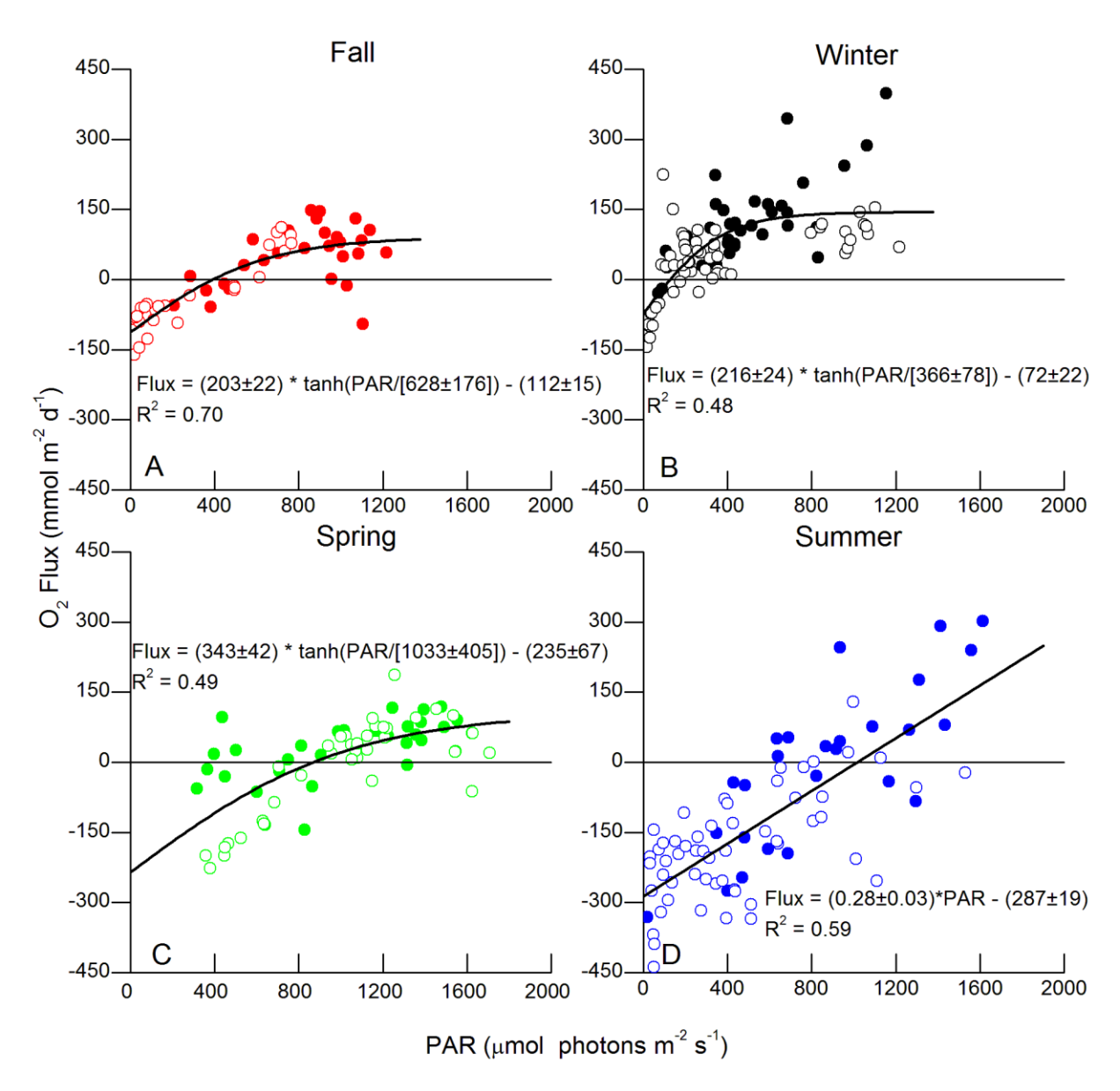
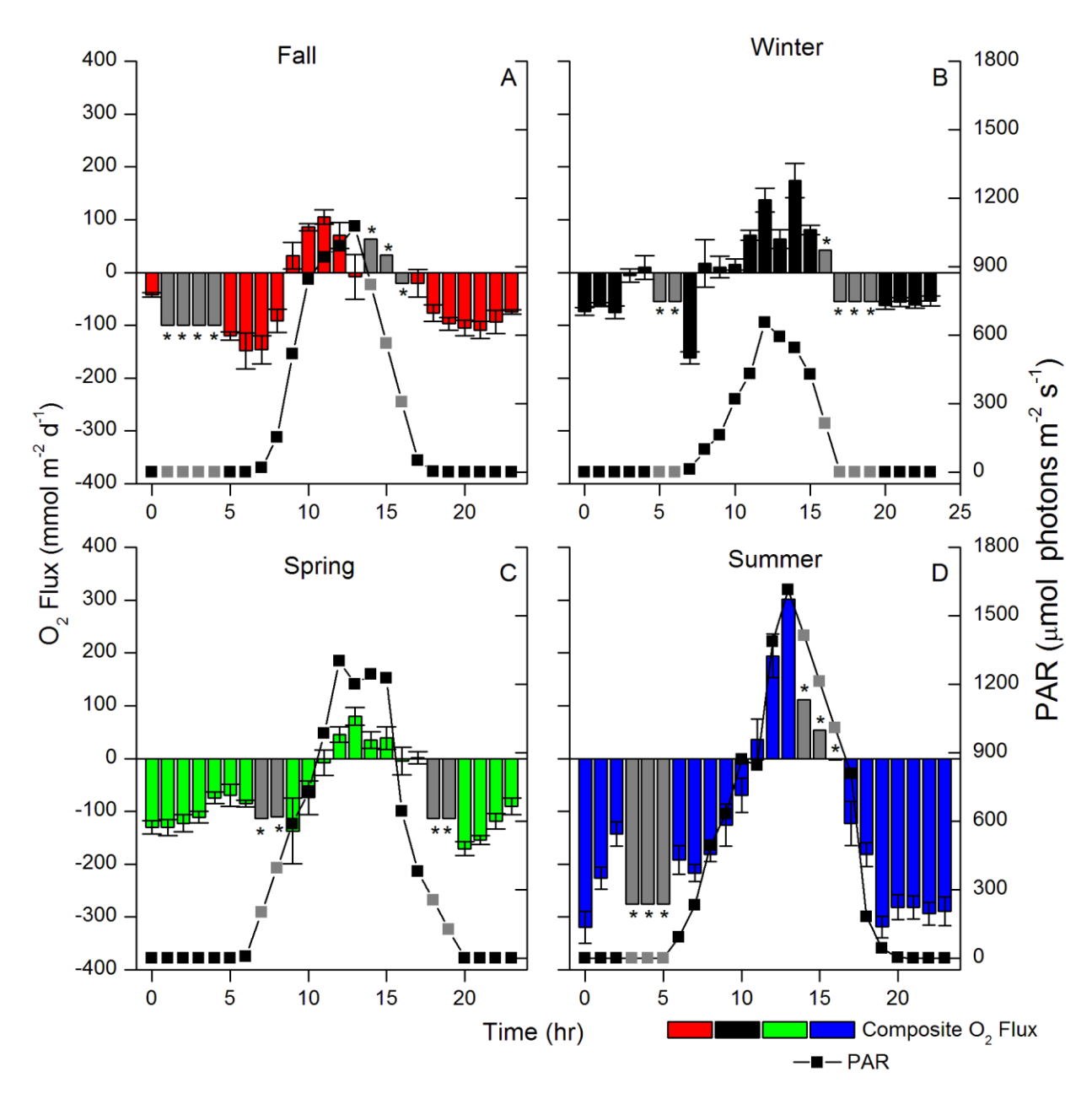


Fig. 3 Seasonal photosynthesis - irradiance (P-I) relationships modeled using a hyperbolic tangential function. Fall, winter, and spring data all showed signs of light saturation, however for summer data the P-I relationship converged to a line. Empty circles represent flood tide fluxes, solid circles represent ebb fluxes. The lack of spring PAR values  $< \sim 400 \mu$ mol photons  $m^{-2}$  s<sup>-1</sup> is due the timing of the tides during these measurements (please see Fig. 4). Values are  $\pm$  SE.



**Fig. 4** Composite daily oxygen flux at the reef during seasonal 2017 measurements. Each column represents the mean of all 15 min values for each hour of the day  $\pm$  SE (n = 1-20), while the squares indicate mean hourly PAR. These composite daily fluxes were used to calculate gross primary production and net ecosystem metabolism for each season. Due to the intertidal nature of the site it was not always possible to record a flux measurement during each hour of the day. In these cases (indicated by asterisks and grey color), daytime hourly flux values were estimated using the P-I relationship from Fig. 3 with PAR that was linearly interpolated based on adjacent values, while nighttime hourly flux estimates were assumed equal to the mean nighttime flux.

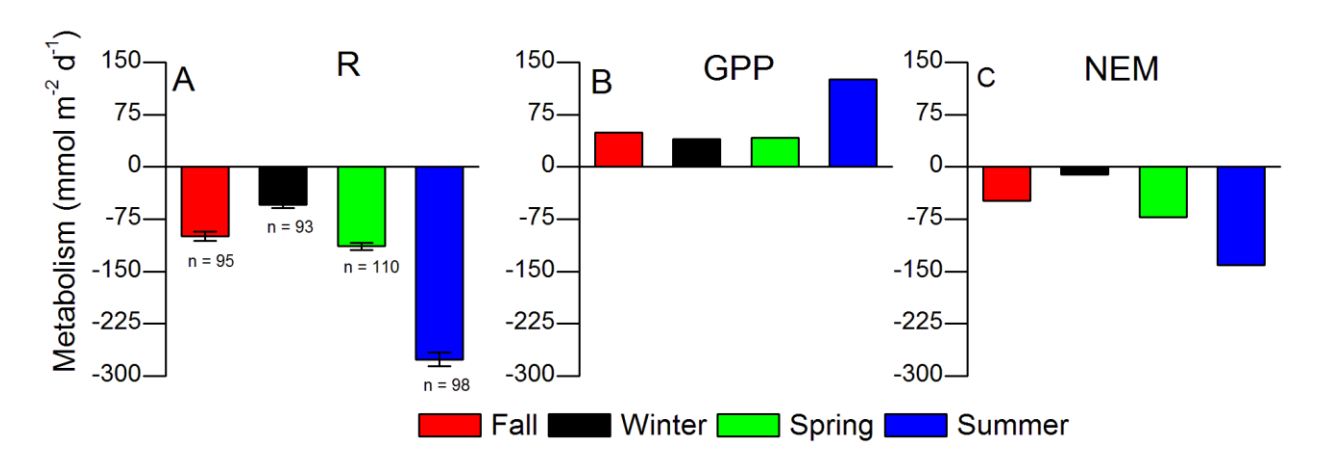
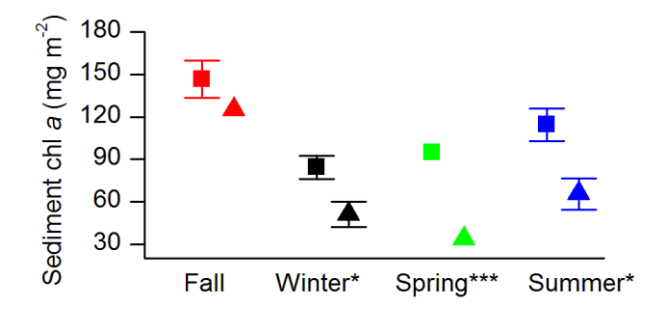


Fig. 5 Seasonal metabolism summary showing (A) ecosystem respiration (R) (B) gross primary production (GPP), and (C) net ecosystem metabolism (NEM). R showed a significant (one-way ANOVA, p < 0.01) seasonal signal, and was highest in the summer and lowest in the winter. GPP was likewise highest in the summer, but was relatively equal across the other three seasons. NEM showed a similar seasonal pattern to R, ranging from nearly balanced in the winter to strong heterotrophy in the summer. Bars represent SE.



**Fig. 6** Sediment benthic chl a for both oyster reef (squares) and control mudflat (triangles). Benthic chl a varied seasonally, and tended to be significantly greater in reef sediments than mudflat sediments (\*p<0.05, \*\*\*\*p<0.001). Bars represent SE, while the absence of bars indicates an error range less than the height of the symbols as plotted (n = 4-10).

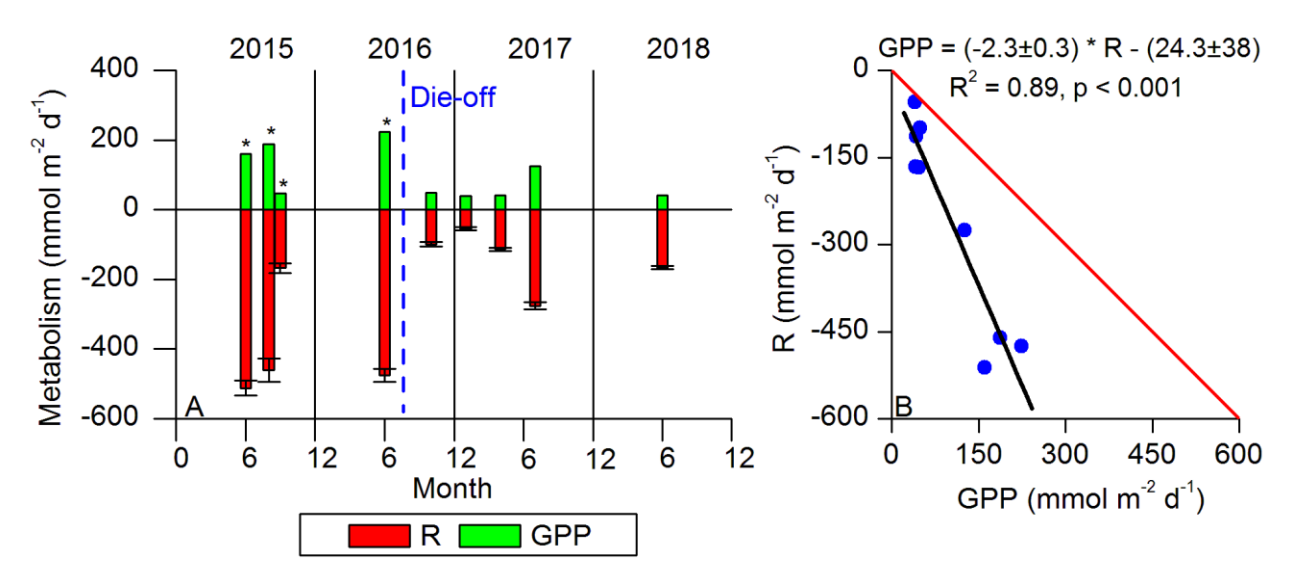


Fig. 7 (A) Four-year record of oxygen metabolism measured at this oyster reef and (B) respiration (R) vs. gross primary production (GPP). Both R and GPP were much higher in 2015-16 than in 2017-18 due to a reef die-off that occurred during late summer 2016. R was highly correlated to GPP, with these values falling below a 1-to-1 line, indicating net heterotrophy on the reef. Asterisks in (A) indicate values adapted from Volaric et al. (2018), with low GPP during Sep 2015 attributed to low PAR during this measurement interval. Bars in (A) represent SE (n = 53-115). Values in (B) are  $\pm$  SE.

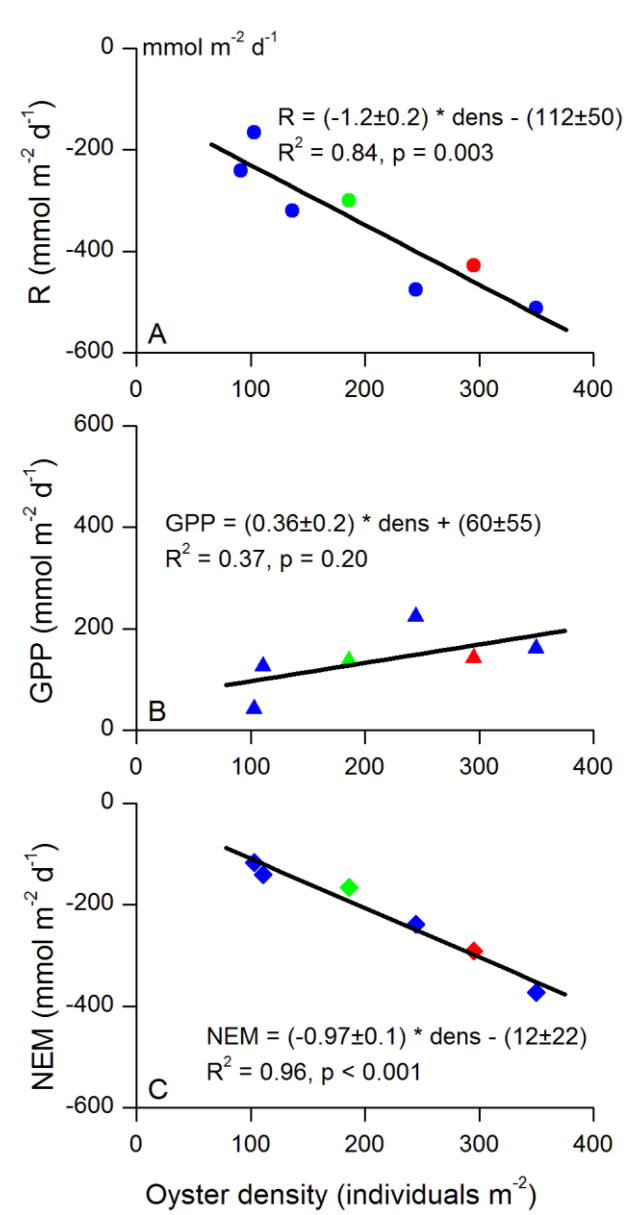


Fig. 8 Summertime (A) ecosystem respiration (R) (B) gross primary production (GPP), and (C) net ecosystem metabolism (NEM) vs. oyster density. Data include past results from this site as well as values from two nearby restored oyster reefs adapted from Volaric et al. (2018) (red and green points). Additionally, both ebb and flood footprint values of R from summer 2017 (Fig. 2) were included in A. Oyster density had a highly significant effect on R and NEM, but had only a weak, nonsignificant impact on GPP. All values are  $\pm$  SE.



**Fig. 9** Image of exposed reef during (A) fall, (B) winter, (C) spring, and (D) summer 2016-2017 measurements. During the winter there was a green alga growing on oyster shells that was not present during other seasons. Oxygen production from this alga, combined with low oyster activity, resulted in winter being the only season that exhibited a nearly balanced net ecosystem metabolism (Fig. 5).